Arch. Mech., **63**, 5–6, pp. 443–457, Warszawa 2011

Three-way actuation of shape memory composite

H. TOBUSHI[1)], S. HAYASHI[2)], E. PIECZYSKA[3)], K. DATE[4)], Y. NISHIMURA[1)]

[1)] *Department of Mechanical Engineering*
Aichi Institute of Technology
1247 Yachigusa, Yakusa-cho
Toyota, 470-0392, Japan
e-mail: tobushi@aitech.ac.jp

[2)] *SMP Technologies Inc.*
Ebisu 1-22-8, Shibuya-ku
Tokyo, 150-0013, Japan

[3)] *Institute of Fundamental Technological Research*
Polish Academy of Sciences
Pawińskiego 5B, 02-106 Warszawa, Poland

[4)] *Ochiai Nexus Co.*
Azamiyama 1-1, Shinpukuji-cho
Okazaki, 444-2106, Japan

The SMC belt composed of two kinds of SMAs with different phase transformation temperatures and SMP, was fabricated and the three-way (reciprocating) movement and recovery force in bending actuation were investigated. The results obtained can be summarized as follows. 1) The three-way bending movement was achived during heating and cooling, based on the characteristics of the SMA tapes and the SMP tape. 2) The recovery force decreased at first and increased thereafter during heating and decreased during cooling. The recovery force was roughly estimated by the proposed model. 3) The development and application of multi-functional SMCs with simple structure for three-dimensional actuators are highly expected.

Key words: shape memory alloy, shape memory polymer, shape memory effect, superelasticity, composite, three-way, bending, recovery force.

1. Introduction

The shape memory alloys (SMAs) are fascinating new functional materials as smart materials [1–3]. The shape memory polymer (SMP) has been also practically used [4–6]. In SMAs, the shape memory property appears based on

the martensitic transformation (MT) in which the crystal structure varies depending on the variation in temperature and stress. In SMAs, the elastic modulus and the yield stress are low at temperatures below the reverse transformation start temperature A_s and high at temperatures above the reverse transformation finish temperature A_f. If SMAs are deformed below A_f, residual strain appears after unloading and the residual strain disappears by heating under no load, showing the shape memory effect (SME). If SMAs are deformed above A_f, strain is recovered during unloading, showing the superelasticity (SE). Strain of 8% is recoverable and the high recovery stress can be used. The properties of energy storage and dissipation can be also used [7]. Among the SMAs, the TiNi SMA shows excellent fatigue strength [8].

In SMPs, the elastic modulus and the yield stress are high at temperatures below the glass transition temperature T_g and low at temperatures above T_g. If SMPs are deformed at temperatures above T_g and cooled down to temperatures below T_g by holding the deformed shape constant, the deformed shape is fixed and SMPs can carry large load. This property is called the shape fixity (SF). If the shape-fixed SMP element is heated up to temperatures above T_g under no load, the original shape is recovered. This property is called the shape recovery (SR). The shape memory property appears based on the glass transition in which the characteristics of molecular motion vary depending on the variation of temperature. Among the SMPs, the polyurethane SMP with sheet, film, foam and other forms has been practically used and strain of several hundred percent is recoverable [9].

In order to use new and higher functions by combining the excellent qualities of both the SMA and the SMP, the development of the shape memory composite (SMC) with the SMA and the SMP is expected [10–13]. If the SMP is used as the matrix in the SMC and the SMA as the fiber, the following properties can be obtained in the SMC. (1) Large recovery force appears, (2) the deformed shape is recovered at high temperature, (3) the deformed shape is held, (4) large load can be carried at low temperature, and (5) the multi-way motion is achieved during heating and cooling. By combining the SMA and the SMP, the SMC element can be developed as demonstrated by TOBUSHI *et al.* [14, 15].

In the present paper, the fabrication and mechanical properties of the SMC belt composed of two kinds of SMAs with different phase transformation temperatures and SMP, which shows the three-way (reciprocating) motion depending on temperature variation, are investigated. With respect to the characteristics of the SMC belt, the bend movement and the recovery force with the three-way property are discussed. The development and application of multi-functional SMC actuator with simple structure are also discussed.

2. Fabrication of SMC belt for three-way motion

2.1. Materials

With respect to the SMAs, two kinds of polycrystalline TiNi alloy tapes showing the SME and SE at room temperature were used. The SMA tape showing the SME was a TiNi alloy tape with a width of 5 mm and a thickness of 0.3 mm, produced by Furukawa Techno Materials Co. The SEA tape showing the SE at room temperature was a TiNi alloy tape with a width of 2.5 mm and a thickness of 0.25 mm produced by Yoshimi Inc. In the shape memory processing, each alloy tape was set along the inside of a fixing ring with an inner diameter of 16 mm and which was heat-treated to memorize the round shape with an outside diameter of 16 mm. The temperature A_f of the SMA tape was 342 K and that of the SEA tape was 309 K. The R-phase transformation finish temperature R_f of the SMA tape was 309 K. These phase transformation temperatures were obtained by the DSC test.

With respect to the SMP, a polyurethane SMP sheet (MM6520) produced by SMP Technologies Inc. was used. The thickness was 0.25 mm and the glass transition temperature T_g was 338 K. The SMP tape with a width of 10 mm was used for the SMC belt.

2.2. Structure and movement properties of SMC belt

The SMC belt with a length of 60 mm, width of 10 mm and thickness of 1.03 mm, was fabricated by using two kinds of alloy tapes and three SMP tapes. In the laminated SMC belt, the SMP tapes were used as a matrix and the alloy tapes as a fiber. The length of the SMA tape and the SEA tape was 50 mm. The SMA tape and the SEA tape were located in the central part of the SMC belt.

The structure of the SMC belt is shown in Fig. 1. It can be seen that the SMA tape and the SEA tape were laminated inside the SMC belt and arranged, facing in the opposite directions for the shape-memorized round shape. The principle of the three-way (reciprocating) bending movement in the SMC belt during heating and cooling is shown in Fig. 2. As it can be seen in Fig. 2, the SMC belt bends to convex downwards (in the direction of the memorized round shape of the SEA tape) by the recovery force of the SEA tape during heating ①–②. It bends to convex upwards (in the direction of the memorized round shape of the SMA tape) by the higher recovery force of the SMA tape at higher temperature ②–③. It regains its original shape during cooling ③–④.

2.3. Fabrication of SMC belt

At first, two incisions were given to one SMP tape and the SMA tape was passed through these incisions. In this process, the SMA tape and SEA tape

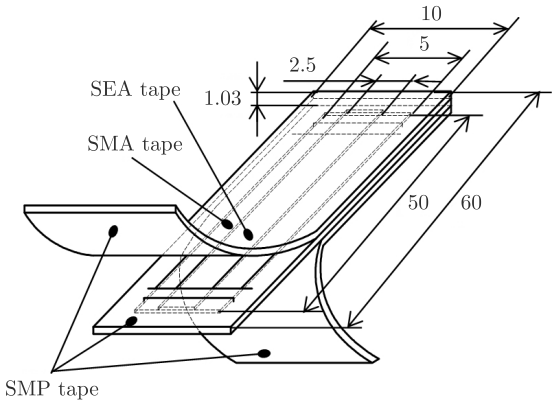

Fig. 1. Structure of SMC belt laminated with SMA tape, SEA tape and SMP tape.

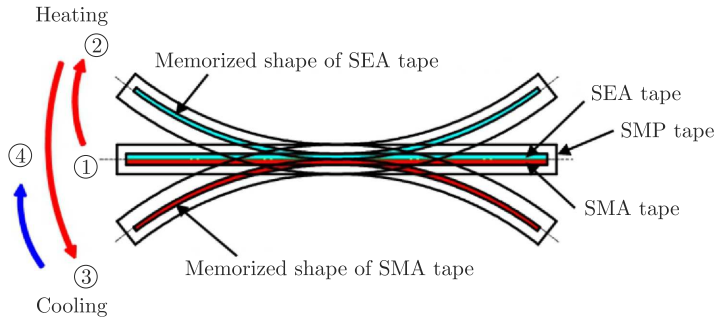

Fig. 2. Principle of three-way bend behavior in SMC belt during heating and cooling.

were arranged facing in the opposite directions for the memorized round shape as shown in Fig. 3. In order to keep the proper positions of both alloy tapes and to protect the projection of the edge by the recovery force of the SMA tape, both edges of the alloy tapes were connected by a thin steel clamp. The SMP tape passed through the SMA tape and the SEA tape were sandwiched between two SMP tapes from upper and lower sides. The laminated material was set in the mold for heat-treating of the SMC belt.

The upper and lower molds were fastened through the bolts by a compressive stress of 7.46 MPa as shown in Fig. 4. The mold was held in the furnace at 448 K for 60 min followed by cooling in air. The laminated SMC belt without bubbles and gaps among the materials could be fabricated under these appropriate conditons: the number of SMP tapes, the fastening force, the heat-treating temperature and time.

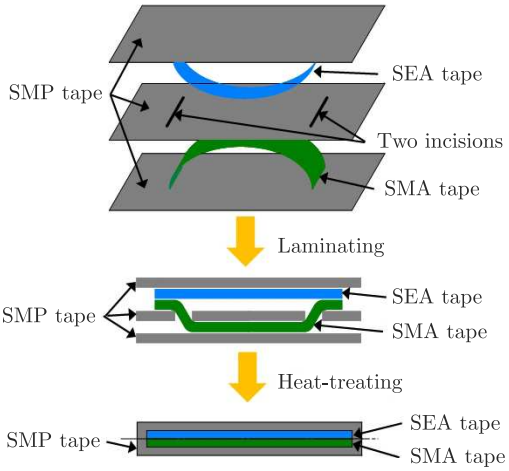

FIG. 3. Arrangements of SMA, SEA and SMP tapes for laminating and heat-treating of the SMC belt.

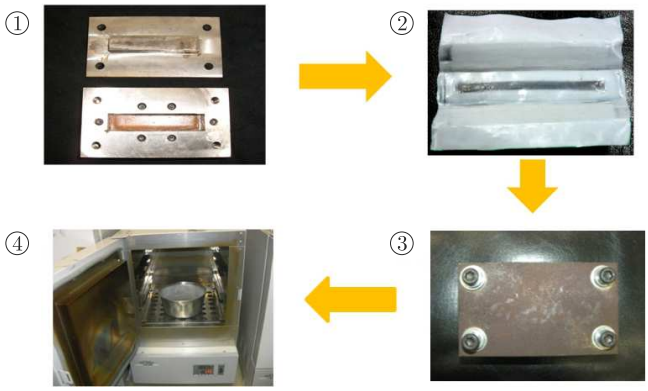

Fig. 4. Photograph of the fabricating the SMC belt: ① upper and lower molds, ② setting the SMC belt on the Teflon sheet, ③ fastening the SMC belt, ④ putting the SMC belt into the furnace for heat treatment.

3. Three-way bending movement of SMC belt

3.1. Three-way bending behavior

The photographs of the three-way (reciprocating) bending motion of the fabricated SMC belt during heating and cooling are shown in Fig. 5. The heating and cooling were carried out between 293 K and 365 K. In Fig. 5, the symbols $A_{f,\mathrm{SEA}}$, $A_{f,\mathrm{SMA}}$, $R_{f,\mathrm{SMA}}$ and T_g represent the reverse-transformation final temperatures of the SEA tape and the SMA tape, the R-phase transformation finish temperature of the SMA tape and the glass transition temperature of the

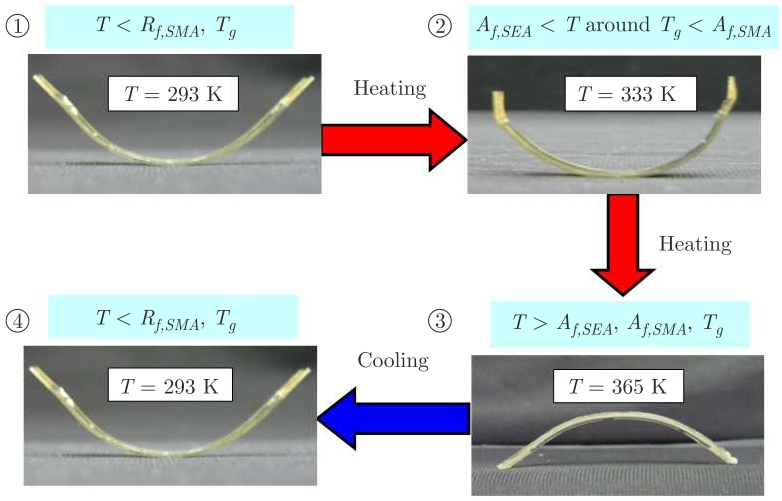

FIG. 5. Photograph of the three-way bending deformation of the SMC belt during heating and cooling.

SMP tape, respectively. At 293 K ①, the internal bending moment induced in the SEA tape is high, and therefore the SMC belt bends in the direction of the shape-memorized round shape of the SEA tape. If the SMC belt is heated ①–②, the SMP becomes soft and the SMC belt bends further to convex downwards (in the same direction at 293 K) at temperatures around T_g ②. If the SMC belt is heated up above T_g ②–③, the SMP becomes easier to deform and the recovery force in the SMA tape increases at temperatures above $A_{f,\mathrm{SMA}}$ and therefore, the SMC belt bends in the direction of the shape-memorized round shape of the SMA tape ③. If the SMC belt is cooled thereafter ③–④, the recovery force in the SMA tape decreases and the recovery force in the SEA tape becomes higher. Therefore, the SMC belt bends again to its original shape ④. This three-way bending motion can be repeated by the cyclic heating and cooling.

3.2. Evaluation of motion based on internal bending moment

The three-way bending motion due to variation in temperature appears based on the variation in the internal bending moment induced in the SEA tape, the SMA tape and the SMP tape in the SMC belt. The internal bending moment can be evaluated as follows. The maximum bending strains of all elements in the three-way movement are calculated by using the radius of curvature and the thickness of each element. The maximum bending strains of the SMA tape, SEA tape and SMP tape were 0.8%, 0.6% and 2.7%, respectively. These strains are in the elastic region of each material and therefore the internal bending moment

of all elements can be evaluated by the theory of elasticity. The internal bending moment M is proportional to the bending rigidity EI and inversely proportional to the radius of curvature r of each element: $M = EI/r$. The dependence of the internal bending moment on temperature can be evaluated as follows. The bending rigidity of the strip is expressed by EI, where E denotes the elastic modulus and I the second moment of area. The internal bending moment of the SMC belt M_c is given by a sum of the internal bending moment in each element as follows:

$$M_C = \frac{E_C I_C}{r_C} = \frac{E_{\mathrm{SEA}} I_{\mathrm{SEA}}}{r_{\mathrm{SEA}}} + \frac{E_{\mathrm{SMA}} I_{\mathrm{SMA}}}{r_{\mathrm{SMA}}} + \frac{E_P I_P}{r_P}, \tag{3.1}$$

where E_C, E_{SEA}, E_{SMA} and E_P denote the elastic modulus of the SMC belt, the SEA tape, the SMA tape and the SMP tape, respectively. I_C, I_{SEA}, I_{SMA} and I_P represent the second moment of area of the SMC belt, the SEA tape, the SMA tape and the SMP tape, respectively. r_C, r_{SEA}, r_{SMA} and r_P denote the radius of curvature of the SMC belt, the SEA tape, the SMA tape and the SMP tape, respectively. There is a following relation for the second moment of area

$$I_C = I_{\mathrm{SEA}} + I_{\mathrm{SMA}} + I_P. \tag{3.2}$$

It should be noticed that the neutral axes of the SMC belt and each element do not coincide. The internal bending moment of the SMC belt is given by the sum of the internal bending moment of each element as expressed by Eq. (3.1). However, in the case of the phase transformation by heating and cooling under no load, the internal bending moment of the SEA element and that of the SMA element act to bend the SMC belt in the opposite direction, to which the round shape of each element was shape-memorized. The internal bending moment in the SMP element acts to bend the SMC belt in the direction of shape-memorized flat shape.

With respect to evaluation of the second moment of area obtained from Eq. (3.2), since the central SMP tape sandwiched between the SEA tape and the SMA tape melts during holding the pressed state at 448 K in the heat-treating process and therefore becomes thin, it can be assumed that the neutral axis of the cross-section in the SMC belt which passes through its centroid coincides with the boundary face between the SEA tape and the SMA tape. Therefore, the neutral axis of the cross-section in each alloy element is located by a distance of $h/2$ from the centroid of the cross-section, and the second moment of area of the alloy element with the width b and height h is $I = bh^3/12 + A(h/2)^2 = bh^3/3$, where the area of the cross-section $A = bh$.

The elastic modulus of the TiNi alloy tape is 70 GPa at temperatures $T > A_f$ and 20 GPa at $T < R_f$. Therefore, the internal bending moment of

the SEA tape $E_{\mathrm{SEA}}I_{\mathrm{SEA}}/r_{\mathrm{SEA}}$ is 118 mN · m at temperatures above 293 K for $r_{\mathrm{SEA}} = 7.9$ mm. $E_{\mathrm{SMA}}I_{\mathrm{SMA}}/r_{\mathrm{SMA}}$ of the SMA tape is 114 mN · m at 293 K and 399 mN · m at 365 K for $r_{\mathrm{SMA}} = 7.9$ mm. The elastic modulus of the SMP tape is 1 GPa at $T < T_g$ and 10 MPa at $T > T_g$. Therefore, the internal bending moment of the SMP tape $E_P I_P/r_P$ is 34.8 mN · m at 293 K for $r_P = 24.5$ mm and 0.249 mN · m at 365 K for $r_P = 34.3$ mm. Based on the temperature dependence of the internal bending moment, the SMC belt moves as follows. At 293 K, the fabricated SMC belt is taken out from the mold, and the SMC belt bends in the direction of the shape-memorized round shape of the SEA tape where the internal bending moment of this element is largest. At 333K around T_g, since the bending rigidity of the SMP tape decreases, that of the SEA tape becomes correspondingly large and therefore the SMC belt bends further in the shape-memorized direction of the SEA tape. At 365 K, the SMC belt bends in the direction of the shape-memorized round shape of the SMA tape where the internal bending moment of this element is the largest.

The three-way movement property of the SMC belt depends on the composition and fraction of the SMA and SMP elements and the rate of heating and cooling processes. For example, if the SMC is cooled rapidly, the SMP element located on the surface is cooled at first and the rigidity of the SMP increases, and therefore the polymer layer becomes hard to deform and the shape at high temperature is fixed. Therefore, in this case, the large recovery movement during cooling can't be obtained by the internal bending moment which appears in the SEA element located inside of the SMC. In order to develop the high-functional SMC actuator, it is necessary to clarify these properties.

3.3. Observation of three-way movement through displacement at the center of SMC belt

The three-way movement was observed through the displacement at the center of the SMC belt. At first, the initial bent-form SMC belt was set on the supports of the three-point bending device in the chamber of the shape-memory characteristics testing machine. After setting the SMC belt, the point of the punch contacted slightly the center of the SMC belt. Keeping the slight contact condition under the contact load lower than 0.1N, the SMC belt was heated and cooled, and the displacement at the center of the SMC belt was measured. The average heating and cooling rates were ±0.02 K/s. The temperature of 365 K was kept constant for 60 min at the end of heating process ③.

The relationship between the displacement at the center of the SMC belt and temperature obtained by the test is shown in Fig. 6. The symbols $A_{f,\mathrm{SEA}}$, $A_{f,\mathrm{SMA}}$, $R_{s,\mathrm{SMA}}$, $R_{f,\mathrm{SMA}}$ and T_g shown in Fig. 6 represent the reverse transformation finish temperatures of the SEA tape and the SMA tape, the R-phase

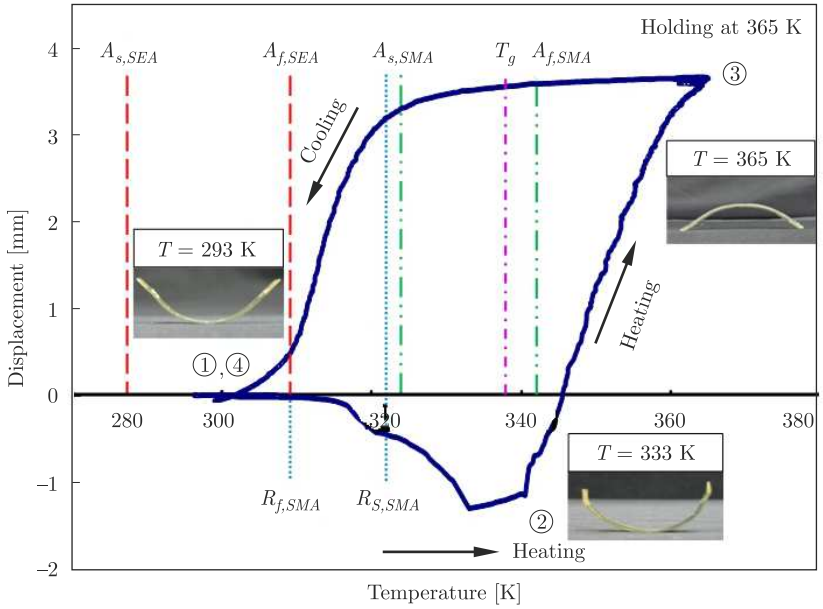

FIG. 6. Relationship between the displacement at the center of the SMC belt supported by two points and temperature during heating and cooling.

transformation start and finish temperatures of the SMA tape, and the glass transition temperature of the SMP tape, respectively. The symbols ①–④ correspond to the deformed states ①–④ shown in Figs. 2 and 5. It should be noticed that if the deflection of the SMC belt increases, the center of the SMC belt moves downwards and the displacement decreases to the negative side. In the heating process ①–②, the displacement at the center of the SMC belt decreases, since the SMP exists in the glass transition region ② and the SMP becomes soft. In the heating process ②–③, the displacement of the SMC belt increases, since the internal bending moment of the SMA tape increases at temperatures above $A_{f,\mathrm{SMA}}$ due to the reverse transformation of the SMA tape. In the cooling process ③–④, the displacement of the SMC belt decreases rapidly at temperatures between $R_{s,\mathrm{SMA}}$ and $R_{f,\mathrm{SMA}}$ since the internal bending moment of the SMA tape decreases and that of the SEA tape becomes higher than that of other elements.

4. Recovery force of SMC belt during heating and cooling

In applications of the SMC belt, we will use not only the bending movement but also the recovery force during heating and cooling [16]. In the present chapter, the recovery force which appears in the SMC belt during heating and cooling will be discussed.

4.1. Three-way behavior of recovery force

In the three-point holding test with heating and cooling for the recovery force, the fabricated SMC belt was put in the supports of the three-point holding device in the chamber of the shape-memory characteristics testing machine. The span was 35 mm. In setting the SMC belt, the center of the SMC belt was put in the punch and the position was held constant. Keeping the positions of the three points (the center and two supports) constant, the SMC belt was heated and cooled. The average heating and cooling rates were ± 0.02 K/s.

The photograph of the three-point holding part of the SMC belt which was kept constant during heating and cooling in the chamber at the recovery force test is shown in Fig. 7.

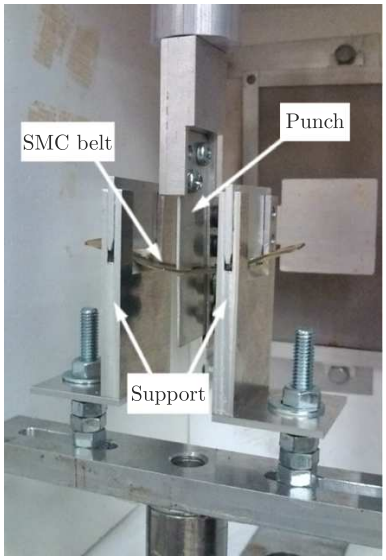

FIG. 7. Photograph of the three-point holding part of the SMC belt in the chamber of the shape-memory characteristics testing machine at the recovery force test.

The relationship between the recovery force at the center of the SMC belt and temperature obtained by the three-point holding test is shown in Fig. 8. The symbols $A_{f,\mathrm{SEA}}$, $A_{f,\mathrm{SMA}}$, $R_{s,\mathrm{SMA}}$, $R_{f,\mathrm{SMA}}$ and T_g shown in Fig. 8 represent the reverse transformation finish temperatures of the SEA tape and the SMA tape, the R-phase transformation start and finish temperatures of the SMA tape and the glass transition temperature of the SMP tape, respectively. The behavior of the recovery force is different between the heating process and cooling process, and the curve describes a large hysteresis loop. In the heating process, since temperatures around the $A_{f,\mathrm{SEA}}$ of the SEA tape are lower than T_g of the SMP tape ①, the elastic modulus of the SMP is high and therefore the rigidity of

the SMP matrix is high. The recovery force of the SMA tape does not appear at this temperature ①, and therefore the recovery force of the SMC is small. Although the elastic modulus of the SMP decreases at temperatures around T_g of the SMP and the deflection of the SMC belt increases, the position of the holding part of the punch is kept constant, and therefore the recovery force of the SMC belt decreases ②. The recovery force starts to increase at temperatures around $A_{f,\mathrm{SMA}}$ of the SMA tape. Since the recovery force of the SMA tape becomes stronger than that of the SEA tape at temperatures around $A_{f,\mathrm{SMA}}$, the recovery force of the SMC belt increases. In the whole heating process, the recovery force of the SMA tape becomes stronger than that of the SEA tape at temperatures above 345 K, and therefore the recovery force of the SMC belt increases rapidly ③.

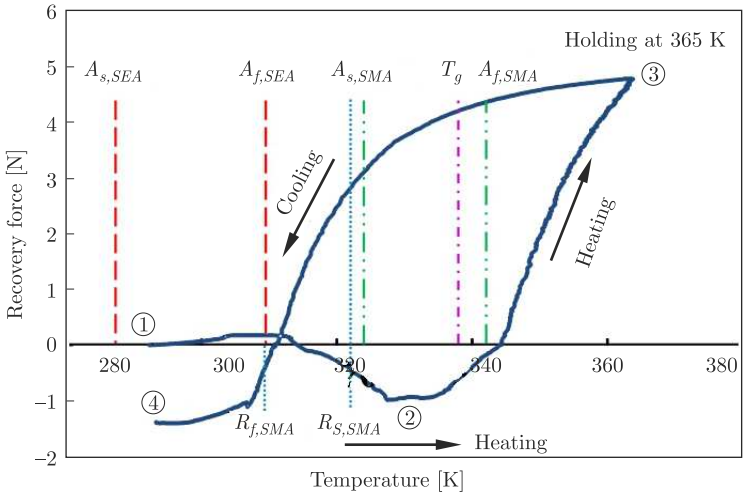

FIG. 8. Relationship between recovery force at the center of the SMC belt and temperature during heating and cooling in the three-point holding test.

In the cooling process, at temperatures around $A_{f,\mathrm{SMA}}$ of the SMA tape, since the recovery force of the SMA tape is higher than that of the SEA tape, the recovery force of the SMC belt decreases gradually. At temperatures around T_g of the SMP, since the recovery force of the SMA tape is higher than that of the SEA tape, the recovery force of the SMC belt is still high. At temperatures from T_g to $R_{s,\mathrm{SMA}}$ of the SMA tape, though the elastic modulus of the SMP becomes high at temperatures below T_g, the recovery force of the SMC belt is 4–3 N since the recovery force of the SMA tape is still strong. At temperatures between $R_{s,\mathrm{SMA}}$ and $R_{f,\mathrm{SMA}}$, the recovery force of the SMA tape decreases rapidly and the recovery force of the SMC belt decreases correspondingly. The recovery force

does not become 0 at the end of cooling ④. It is necessary to clarify the reason. The cyclic deformation properties and the shear strength of interfaces among each element are also the future work.

4.2. Evaluation of recovery force

The recovery force at high temperature can be evaluated as follows. In the case of small deflection, the deflection y at the center of the SMC belt in the three-point bending is given by the following equation

$$y = \frac{Wl^3}{48E_cI_c}, \tag{4.1}$$

where W and l denote the load applied at the center and the span, respectively. Therefore, the recovery force at the center of the SMC belt F_r at high temperature for the displacement at the center y_C is obtained by the following equation

$$F_r = \frac{48E_cI_c}{l^3}y_C. \tag{4.2}$$

The internal bending moment which appears to bend the SMC belt at 365 K is as follows. Although the internal bending moment in the SMA tape acts in the direction in which the SMC belt bends to convex upwards, the internal bending moment in the SEA tape acts to the opposite direction in which the SMC belt bends to convex downwards. Therefore, from Eq. (3.1), the bending rigidity of the SMC belt is obtained as $E_cI_c = 4015\ \mathrm{N}\cdot\mathrm{mm}^2$. Substituting the measured values of $l = 35$ mm and $y_C = 1.99$ mm in Eq. (4.2), the variation in the recovery force F_r from low temperature to high temperature is 8.94 N. This value is larger than the measured variation in the recovery force of 6 N by about 50%. The recovery force induced at the center of the SMC belt in the three-point holding can be roughly estimated by Eq. (4.2). Equations (4.1) and (4.2) are obtained in the case of small deflection for the three-point bending with a concentrated load at the center of the belt. However, the rather uniform internal bending moment can appear in the SMC belt. The analysis of the recovery force in the SMC belt based on the uniform internal bending moment for large deflection is the future work.

5. Development of multi-functional SMC actuator

The SMC belt frabricated in the present paper shows the three-way bend properties during heating and cooling. The SMC belt was composed of two kinds of SMAs with different phase transformation temperatures and SMP. The glass

transition temperataure of the SMP was between the phase transformation temperatures of the SMAs. The thermomechanical properties of SMC vary depending on the combination of the SMA and the SMP with various phase transformation temperatures, volume fractions, structural compositions and heating-cooling rates. Therefore, various kinds of multi-way actuators can be developed by using these combinations. The cyclic deformation properties and strength of the interfaces between the alloy and the polymer are important for development of SMC actuators. They are the future subjects.

The three-way bend behavior observed in the SMC belt was in the same plane. The axes of the SMA tapes with different phase transformation temperatures were in the same direction in the SMC belt. If the axes of the SMA tapes in the SMC sheet are arranged in various directions, the SMC sheet bends in the various planes. That is, the three-dimensional actuations can be obtained by using these compositions.

Therefore the development and application of multi-functional SMC actuators with simple structure for the three-dimensional motion are highly expected.

6. Conclusions

The SMC belt composed of two kinds of SMAs with different phase transformation temperatures and SMP was fabricated and the three-way bending movement and recovery force were investigated. The results obtained can be summarized as follows.

1. Two kinds of TiNi alloy tapes showing the SME and SE were heat-treated to memorize the round shape, respectively. The shape-memorized round alloy tapes were arranged facing in the opposite direction and were sandwiched by one SMP tape in the central part and by two SMP tapes from upper and lower sides. The laminated SMC belt was fabricated without bubble and gap by using the appropriate factors: the number of SMP tapes, the fastening force, the heat-treating temperature and time.

2. The three-way bend movement was achieved during heating and cooling based on the characteristics of the alloy tapes and the SMP tape.

3. The recovery force at the center of the SMC belt in the three-point holding test decreased at first and increased thereafter during heating and decreased during cooling. The recovery force was roughly estimated by the proposed model.

4. The development and application of multi-functional SMCs with simple structure for three-dimensional actuators are highly expected by the combination of the SMAs and the SMPs with various kinds of phase transformation temperatures, volume fractions, compositions and heating-cooling rates.

Acknowledgements

This study was performed as a part of the bilateral joint research project between Aichi Institute of Technology and Institute of Fundamental Technological Research, Polish Academy of Sciences, supported by the Japan Society for Promotion of Science and Polish Academy of Sciences. The experimental work for this study was carried out with the assistance of students from Aichi Institute of Technology, to whom the authors wish to express their gratitude. The authors are also grateful to the administrators of Scientific Research (C) in Grant-in-Aid for Scientific Research by the Japan Society for Promotion of Science and The Naito Research Grant for financial support. The research was also partly supported by the Polish Ministry of Science and Higher Education under Grant No 501220837.

References

1. H. Funakubo [Ed.], *Shape memory alloys*, Gordon and Breach Science Pub., 1–60, 1987.
2. T.W. Duerig, K.N. Melton, D. Stockel, C.M. Wayman [Eds.], *Engineering Aspects of Shape Memory Alloys*, Butterworth-Heinemann, 1–35, 1990.
3. K. Otsuka, C.M. Waymam [Eds.], *Shape Memory Materials*, Cambridge University Press, 1–49, 1998.
4. S. Hayashi, *Properties and applications of polyurethane series shape memory polymer*, Int. Progr. Urethanes, **6**, 90–115, 1993.
5. H. Tobushi, T. Hashimoto, N. Ito, S. Hayashi, E. Yamada, *Shape fixity and shape recovery in a film of shape memory polymer of polyurethane series*, J. Intell. Mater. Syst. Struct., **9**, 127–136, 1998.
6. H. Tobushi, S. Hayashi, K. Hoshio, Y. Ejiri, *Shape recovery and irrecoverable strain control in polyurethane shape-memory polymer*, Sci. Technol. Adv. Mater., **9**, 1–7, 2008.
7. E.A. Pieczyska, S. Gadaj, W.K. Nowacki, K. Hoshio, Y. Makino, H. Tobushi, *Characteristics of energy storage and dissipation in TiNi shape memory*, Sci. Tech. Advanced Mater., **6**, 889–894, 2005.
8. H. Tobushi, T. Hachisuka, T. Hashimoto, S. Yamada, *Cyclic deformation and fatigue of a TiNi shape-memory alloy wire subjected to rotating bending*, Trans. ASME, J. Eng. Mater. Tech., **64**, 64–70, 1998.
9. H. Tobushi, E.A. Pieczyska, Y. Ejiri, T. Sakuragi, *Thermomechanical properties of shape-memory alloy and polymer and their composite*, Mech. Advanced Mater. Struct., **16**, 236–247, 2009.
10. T. Sterzl, B. Winzek, M. Mennicken, R. Nagelsdiek, H. Keul, H. Hocker, E. Quandt, *Bistable shape memory thin film actuators*, Smart Structures and Materials 2003, Proc. SPIE, **5053**, 101–109, 2003.
11. M. Kawai, *Shape memory alloy composites*, J. JSEM, **6**, 4, 363–372, 2006.

12. J.E. MANZO, E. GARCIA, *Active rigidity smart joint for a bat-wing micro air vehicle*, Proc. IMECE, **43065**, 231–241, 2007.

13. BROWNE *et al.*, *Programmable Shims for Manufacturing and Assembly Lines*, US7538472B2, U.S. Patent, 2009.

14. H. TOBUSHI, S. HAYASHI, K. HOSHIO, Y. MAKINO, N. MIWA, *Bending actuation characteristics of shape memory composite with SMA and SMP*, J. Intell. Mater. Syst. Struct., **17**, 1075–1081, 2006.

15. H. TOBUSHI, S. HAYASHI, Y. SUGIMOTO, K. DATE, *Two-way bending properties of shape memory composite with SMA and SMP*, Materials, **2**, 1180–1192, 2009.

16. P.H. LIN, H. TOBUSHI, K. TANAKA, C. LEXCELLENT, A. IKAI, *Recovery stress of TiNi shape memory alloy under constant strain*, Arch. Mech., **47**, 281–293, 1995.

Received November 10, 2010; revised version March 18, 2011.